

Hydroxymethylnitrofurazone (NFOH) decreases parasitaemia, parasitism and tissue lesion caused by infection with the Bolivia *Trypanosoma cruzi* type I strain in Swiss and C57BL/6 mice

Cauê Benito Scarim^{1*}, Cleverton Roberto de Andrade², Rossana Falcone³,
Leticia Moreno Ambrozini³, Vitor Izidoro Senhorelli¹,
João Aristeu da Rosa³, Chung Man Chin¹

*1*Sao Paulo State University “Júlio de Mesquita Filho”, UNESP, Faculty of Pharmaceutical Sciences, Department of Pharmaceuticals and Medicines, Araraquara, SP, Brazil, *2*Sao Paulo State University “Júlio de Mesquita Filho”, UNESP, Faculty of Dentistry, Department of Physiology and Pathology, Araraquara, SP, Brazil, *3*Sao Paulo State University “Júlio de Mesquita Filho”, UNESP, Faculty of Pharmaceutical Sciences, Department of biosciences and biotechnology, Araraquara, SP, Brazil

The chemical hydroxymethylation of the antimicrobial nitrofurazone leads to the prodrug NFOH, also increases the anti-*T. cruzi* activities (*in vitro* and *in vivo*), as well as showed non-genotoxic (Ames and micronucleus assays). In the present study, we assessed the anti-*T. cruzi* effect of the NFOH *In vivo* - in acute Swiss and C57Bl/6 experimental Chagas models. The treatment started at 5 days post-infection during 20 consecutive days (orally, once day, 150mg/kg), and the parasitaemia as well as histopathology analysis were performed. In both experimental murine models, NFOH was able to reduce parasitemia blood avoiding parasitic reactivation, during immunosuppression period (dexamethasone 5mg/kg, 14 days), in 100% of the mice, and decrease tissue parasite nests, demonstrating absence of amastigote forms in all organs (100%) analyzed, data similar to benznidazole (BZN). Therefore, the results shown here pointing to the NFOH as promising compound for further preclinical studies, being a high potential drug to effective and safe chemotherapy to Chagas disease.

Keywords: Chagas disease. *Trypanosoma cruzi*. Bolivia strain. Acute stage. Hydroxymethylnitrofurazone (NFOH). Benznidazole (BZN).

INTRODUCTION

Chagas disease (also known as American trypanosomiasis) is a public health problem in Mexico, and Central and South America, it directly causes around 14,000 deaths each year¹⁻³. Moreover, this tropical disease affects more than six million people worldwide. It is caused by the etiologic agent *Trypanosoma cruzi* (*T. cruzi*) (DNDi, 2018; Chagas, 1909; Lidani *et al.*, 2019).

Chemotherapy drugs are nitro-compounds: nifurtimox and benznidazole (BZN) (DNDi, 2018; Lidani *et al.*, 2019), developed in the 1960s and 1970s, respectively (Castro, de Mecca, Bartel, 2006; Maya *et al.*, 2010). Both drugs are, mostly, actives in the acute stage of human treatment, eradicating trypomastigote forms. Nevertheless, these nitro-compounds exhibited limited effects in chronic stage of Chagas disease²¹⁻²⁵. Moreover, nitro-compound demonstrated various significant adverse events when used during long-term therapy (Andrade *et al.*, 1996; Andrade *et al.*, 2013; Fernandes *et al.*, 2009; Fernandez *et al.*, 2016; Hasslocher-Moreno *et al.*, 2012; Silva *et al.*, 2014; Sosa-Estani *et al.*, 1998; Soy *et al.*, 2015). No new drugs have established safe and effective use for both Chagas stages (acute and chronic

*Correspondence: C. B. Scarim. Faculdade de Ciências Farmacêuticas (UNESP). Departamento de Fármacos e Medicamentos. Universidade Estadual Paulista “Júlio de Mesquita Filho”. Rodovia Araraquara- Jaú km 1. CEP 14801903, Araraquara, São Paulo, Brasil. Phone: +55 (16)3301 6962. E-mail: cauebenitos@gmail.com. ORCID: 0000-0002-2540-6395

phases) (Castro, de Mecca, Bartel, 2006; Maya *et al.*, 2010), therefore, there is an urgent need for the development of new drugs for future therapeutic alternatives.

Hydroxymethylnitrofurazone (NFOH, a nitro-compound) is a nitrofurazone prodrug that has demonstrated *in vitro* (Chung *et al.*, 2003) and *in vivo* (Davies *et al.*, 2010; Scarim *et al.*, 2018a) activities against *Trypanosoma cruzi* (*T. cruzi*) parasites. NFOH displayed significant inhibition of both human forms of *T. cruzi* (amastigote and trypomastigote forms) in assays (Chung *et al.*, 2003). Furthermore, NFOH is non-genotoxic (in Ames tests) (Guido *et al.*, 2001) and non-hepatotoxic after short (21 days) and long (60 days) treatment periods (Scarim *et al.*, 2018a; Davies *et al.*, 2014). Moreover, NFOH exhibited approximately 20 times more volume distribution than nitrofurazone in rats (Serafim *et al.*, 2013), and 10% more distribution in rabbits (Nogueira-Filho *et al.*, 2013).

Davies and collaborators (2010) detected a sterile cure (PCR-based methodology) in Swiss mice infected with the Tulahuen strain of *T. cruzi*. They established negative PCR in 100% of the mice 180 days after the last NFOH treatment dose (150 mg/kg, 60 days) that started at 5 dpi (days post infection). Besides that, 78.5% of mice treated with NFOH (50 mg/kg) reported parasitaemia elimination after four days of treatment using *T. cruzi* Brazil Luc strains in an experimental assay (Ekins *et al.*, 2015). Histopathological analysis demonstrated that NFOH (150 mg/kg/day) decreased the intensity of tissue amastigote and inflammatory infiltrate when compared to BZN (100 mg/kg/day) in the indeterminate chronic phase of experimental Chagas disease (Y strain) (Scarim *et al.*, 2018a). Thus, this *in vivo* data corroborates to previous *in vivo* assays using three different *T. cruzi* strains (Tulahuen⁴¹, Brazil luc⁴³ and Y⁵⁴) (Davies *et al.*, 2010; Ekins *et al.*, 2015; Scarim *et al.*, 2018a), which encouraged us to verify NFOH activity *in vivo* using two murine models during acute stage of CD infection.

Therefore, the general objective of this research was to identify the potential of NFOH-therapy in preventing parasitaemia reactivation, decrease the inflammation and tissue parasitism during the acute stage. This was performed by histopathological analysis of six organs (heart, skeletal muscle, colon, liver, kidney, and spleen) of mice previously infected with the Bolivia strain of *T. cruzi*.

MATERIAL AND METHODS

Animal models

In this work, Swiss and C57Bl/6 male mice (20-25g, age of approximately one month) were maintained under controlled temperatures (23±1 °C) and humidity (55±5 %), and automatic lighting (12/12 hour cycles). They were fed and given water *ad libitum*. All the procedures conducted in this experiment were approved by the Research Ethics Committee of Animal Experimentation of the School of Pharmaceutical Sciences of Araraquara, São Paulo State University (UNESP) (CEUA/FCF/CAr: 28/2018), Brazil.

Experimental protocol

The infection was standardized and performed in the Parasitology Laboratory of the School of Pharmaceutical Sciences, São Paulo State University (UNESP), Araraquara, São Paulo, Brazil. The mice were infected with *T. cruzi* (intraperitoneal injection – blood transfusion) by an inoculum of (1x10²) trypomastigote forms of the Bolivia strain. Here, we monitored the parasitaemia during all protocols, according to Scarim and co-workers (2018a). Brener's technique was used. For both murine models, three infected groups were separated. The groups included an infected non-treated group (only vehicle, once day) (INT), an infected BZN-treated group (IBZN, 100 mg/kg once day), an infected NFOH-treated group (INFOH, 150 mg/kg once day), and a non-infected and non-treated (NI) group (only vehicle, once day) (N = 30 by murine experiment; each infected group, n = 8; each non-infected group, n = 6). The drugs were administrated orally in a suspension of arabic gum (4%) once a day for 20 consecutive days. Throughout the experiment, the weight of the mice was monitored and measured weekly to identify weight alterations and protocol changes. At the end of the experiment (after euthanasia, CO₂ saturation euthanasia), the organs were weighed to establish their relative weights according to the following equation (Equation 1):

$$\text{Equation 1} = \text{Relative weight (\%)} = \left(\frac{\text{[organ/mice weight]}}{\text{[organ/mice weight]}} \times 100 \right)$$

Histopathology

After euthanization, the organs were collected and fixed in tamponed formaldehyde (10%). After approximately 24 hours, they were included in paraffin and sliced in 4µM. After this, they were stained in Hematoxilin & Eosin. Two trained analysts, as part of a blind evaluation, examined the results using serial sections of 3 mm diameter in two different moments.

Thus, the parameters of analysis were described by Scarim and co-workers (2018a) (Tables I - III). For statistical analysis, GraphPad Prism Software® (La Jolla, CA, USA) statistical program 8.1 was used with the application of variance analysis ($p < 0.05$) by Tukey's multiple comparison test and the ANOVA parametric test. These were performed using analysis from the Kruskal-Wallis nonparametric test ($p < 0.05$).

TABLE I - Numerical criteria for the classification of inflammatory parameters according to the type of cell found during histopathological analysis

Infiltrates parameters	Intensity				Type		
	Absent (0%)	Mild (1-33%)	Moderate (33 – 66%)	Intense (> 66%)	Acute	Mixed	Chronic
Inflammatory Infiltrates	-1	0	1	2	-1 - 0	0.1 - 1	1.1 - 2

TABLE II - Numerical criteria for the classification of hepatic parameters according to the type finding during histopathological analysis

Lymphoid parameters (spleen)	Decreased		Increased	
	White pulp	0.1 - 1	1.1 - 2	
Red pulp	0.1 - 1	1.1 - 2		
Lymphoid follicles	Disorganized		Organized	
	-1 - 0	0.1 - 1		

TABLE III - Numerical criteria for the classification of splenic parameters according to the histopathological.

Hepatic parameters (Liver)	Intensity			
	Absent (0%)	Mild (1-33%)	Moderate (33 – 66%)	Intense (> 66%)
Calcification	-1	0	1	2
Necrosis	-1	0	1	2
Amastigote nests	-1	0	1	2

Statistical analysis

For statistical analysis, GraphPad Prism Software® (La Jolla, CA, USA) statistical program 8.1 was used by applying analysis of variance by Student's t-test or one-way ANOVA, with Tukey's post-hoc correction in GraphPad Prism v.7. Differences of $p < 0.05$ were considered significant.

RESULTS AND DISCUSSION

Parasitaemia and relative weights

The parasitaemia curves and weights are shown in Figure 1A-D. For the Swiss mice protocol, the acute stage lasted for about 91 dpi in the INT, 11 dpi in the IBZN groups, and 13 dpi for the INFOH mice (Figure 1A). No mice died during this part of the experiment. The pre-patent period was shorter than 5 dpi for all infected groups (INT, IBZN, INFOH), and the parasitemic peak in the INT group was identified at approximately 11-13 dpi, showing similar to the IBZN and INFOH mice at 7 dpi. Thus, there was statistical difference between the IBZN and INFOH groups when compared to the INT from 11 dpi until 91 dpi (Figure 1A).

In C57Bl/6 mice, the acute stage lasted until approximately 91 dpi for the INT, 13 dpi for IBZN groups, and 15 dpi for the INFOH mice (Figure 1B). The pre-patent period was shorter than 5 dpi for all infected groups (INT, IBZN, INFOH). The parasitemic peak was identified in the INT group at approximately 9-11 dpi, 7 dpi in the infected IBZN mice, and 9 dpi in the infected INFOH mice (Figure 1B). No mice died in the NI, IBZN, and INFOH groups during the experiment, however, three mice (37.5%) in the INT group died.

Through the monitoring of relative body weight in the treatment period of Swiss mice, the INT displayed weight gain that was statistically different than the other groups ($p < 0.05$) (Figure 1C). On the other hand, the INFOH showed increased detachment and weight gain at 28 and 56 dpi when compared to the IBZN and NI ($p < 0.05$) groups, as well as at 84 dpi ($p < 0.05$) when compared to all other groups (Figure 1C). For the C57Bl/6 mice, the INT and NI groups exhibited differences ($p <$

0.05) when compared to the IBZN and INFOH groups at 7 dpi. At 14 dpi, the INT mice demonstrated statistical difference when compared to the other groups ($p < 0.05$) (Figure 1D). At 21 and 28 dpi, the INT and NI groups displayed differences ($p < 0.05$) when compared to treated groups, IBZN and INFOH mice. At 70 dpi, the NI mice showed statistical difference ($p < 0.05$) presenting a decrease in the relative body weight when compared to all infected groups (INT, IBZN, INFOH, Figure 1D). Moreover, in the final three weeks (at 77, 84, and 91 dpi), the INT and IBZN groups exhibited statistical differences ($p < 0.05$) showing a reduction in the relative body weight when compared to the INFOH and NI groups (Figure 1D).

At 91 dpi, we performed relative weight analysis of the organs of the Swiss mice (heart, visceral fat, liver, kidney, skeletal muscle, and spleen) (Figure 1E). In the liver, all infected groups displayed hepatomegaly when compared to the NI (INT, $p = 0.0345$; IBZN, $p = 0.0429$; INFOH, $p = 0.0108$) (Figure 2A). Furthermore, we observed statistical differences in hepatic weight in the IBZN and INT ($p = 0.0023$) (Figure 1E), however, there were no differences between IBZN and INFOH groups. The renal relative weight demonstrated statistical differences in the NI mice when compared to the INT ($p = 0.0164$) and INFOH ($p = 0.0002$) groups. Moreover, there were no differences between the IBZN and INFOH groups. For skeletal muscle, all infected groups exhibited increases of relative weight when compared to the NI (INT, $p < 0.0001$; IBZN, $p = 0.0001$; INFOH, $p = 0.0001$) (Figure 1E). Concerning splenic relative weight, two infected groups (INT, $p = 0.0008$; INFOH, $p = 0.0002$) displayed splenomegaly when compared to the NI. The IBZN was an exception. Therefore, there were differences between the IBZN and INFOH ($p = 0.0014$). Statistical differences were also identified in splenic relative weight between the IBZN and INT ($p = 0.0002$) groups (Figure 1E). The other organs, heart and visceral fat, did not show any differences concerning relative weight (Swiss mice).

At 91 dpi, the relative weights of the hearts and visceral fat tissues of C57Bl/6 mice did not show significant differences between analyzed groups (Figure 1F). For the liver, the infected groups displayed hepatomegaly when compared to the INT ($p = 0.0248$), IBZN ($p = 0.0004$), and INFOH ($p = 0.0005$) (Figure 1F), nevertheless, there were

no differences between the IBZN and INFOH. The relative kidney weight of the NI showed a statistical difference when compared to the INT ($p = 0.0068$), IBZN ($p = 0.0216$), and INFOH ($p = 0.0002$). Additionally, there were no differences between the IBZN and INFOH concerning relative kidney weight. In skeletal muscle relative weight, all infected groups demonstrated increases of relative weight compared to the NI (INT, $p < 0.0015$; IBZN, $p = 0.0367$;

INFOH, $p = 0.0433$) (Figure 1F). Likewise, statistical differences were observed in relative weight of the skeletal muscle in the NI, IBZN ($p < 0.0001$), and INFOH ($p < 0.0001$) (Figure 1F). For the splenic relative weight, all infected groups presented splenomegaly when compared to the NI (INT, $p = 0.0118$; IBZN, $p = 0.0250$; INFOH, $p < 0.0001$). Thus, we also observed differences between the IBZN and INFOH ($p = 0.0404$) (Figure 1F).

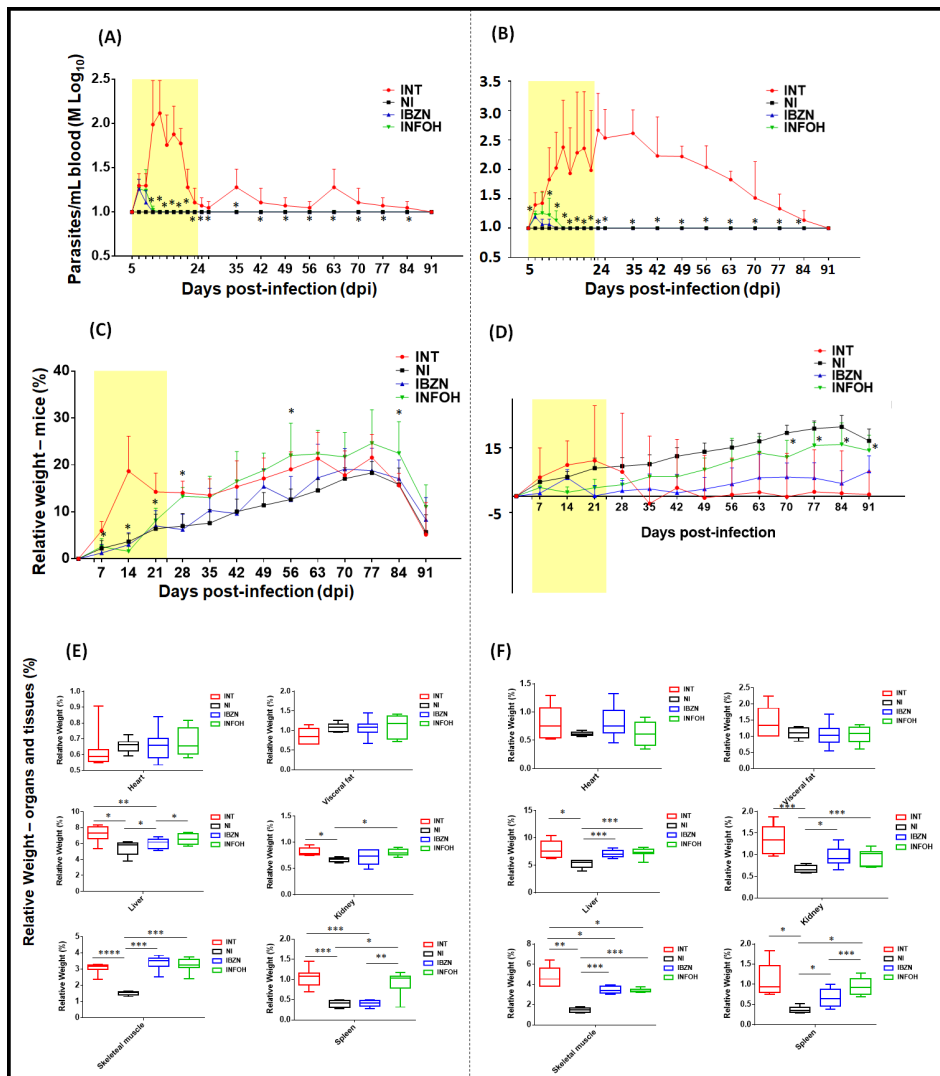


FIGURE 1 - Parasitaemia and relative weight monitoring in two different murine models (Swiss and C57BL/6). (A, B) *T. cruzi* TcI (Bolivia strain) parasitaemia curves from infected mice (INT, IBZN, and INFOH) are expressed as logarithmic means (M log₁₀). The treatment period is highlighted in yellow (20 days: BZN 100mg/kg and NFOH 150 mg/kg). The data are expressed as averages of ± SD. *Statistically significant difference ($p \leq 0.05$). (C, D) Relative weight during protocol. (E, F) Relative weight of the organs (heart, visceral fat, liver, kidney, skeletal muscle, and spleen). INT: infected non-treated group, only vehicle; NI: non-infected group, only vehicle; IBZN: infected and treated with benznidazole; INFOH: infected and treated with hydroxymethylnitrofurazone. The data are expressed as averages of ± SD. Analysis of variance by Student's t-test or one-way ANOVA, with Tukey's post-hoc correction in GraphPad Prism v.7. Differences of $p < 0.05$ were considered significant. *Statistically significant difference ($p \leq 0.05$); **Statistically significant difference ($p \leq 0.005$); ***Statistically significant ($p \leq 0.0005$); The data are expressed as averages of ± SD.

Histopathology

The general results of complex histopathological analyses of the Swiss murine models are displayed in Figure 2A. Representative histological images are shown in Figure 3A. Although the NI presented less outward inflammatory infiltrates in the heart tissue when compared to the INT, IBZN, and INFOH groups, nonetheless, statistical differences were not verified. The INT mice was the only group that presented amastigote forms of *T. cruzi* in the cardiac tissue. These were absent in the treated mice, IBZN and INFOH groups. Therefore, calcification and necrosis areas were observed in the INT and IBZN groups, but without statistical difference (Figure 2A).

In the skeletal muscle, high presences of inflammatory infiltrates, calcification, and necrosis were observed in the INT when compared to the NI, IBZN, and INFOH groups. However, the presence of amastigote forms (absent in IBZN and INFOH) did not demonstrate differences (Figure 2A). Similarly, we identified high levels of infiltrates, necrosis, and amastigotes in colon tissues of the INT mice. These levels were not found in the NI, IBZN, and INFOH groups. The INT showed more hepatic inflammatory tissue than all other groups (NI, $p < 0.0001$; IBZN, $p < 0.0001$, INFOH, $p < 0.0001$) (Figure 2A). In addition, The IBZN demonstrated a greater amount of hepatic inflammatory infiltrates than the INFOH ($p < 0.0001$) and NI ($p < 0.0001$) groups. Moreover, we identified the presence of calcification, necrosis areas, and amastigote nests in the liver of the mice in the INT mice, while was not observed in IBZN

and INFOH groups. Differences in the histopathological analysis of the spleen and kidney were not observed when comparing all groups (Figure 2A).

The results of the histological analysis of the C57Bl/6 mice are exhibited in Figure 2B, and their representative histopathological photography are shown in Figure 3B. The NI group exhibited the lowest amount of inflammatory infiltrates in cardiac tissue when compared to all infected groups (INT, IBZN, INFOH, Figure 2B). In the skeletal muscle, we observed a high presence of inflammatory infiltrates, calcification, and necrosis in the INT when compared to the NI, IBZN, and INFOH groups. We also observed an absence of amastigote forms in the IBZN and INFOH.

In the colon, we identified high quantities of infiltrates in the INT when compared to other groups, showing statistical difference when compared to the NI ($p = 0.0363$). An area of necrosis was found in the INT and IBZN groups. Amastigote presence was identified in the INT, demonstrating a difference when compared to all the other groups (NI, $p = 0.0363$; IBZN and INFOH, $p = 0.0209$). The INT showed more hepatic inflammatory tissue than all the other groups (NI, $p < 0.0001$; IBZN, $p < 0.0001$, INFOH, $p < 0.0001$) (Figure 2B). The IBZN demonstrated a greater amount of hepatic inflammatory infiltrates than the INFOH ($p < 0.0001$) and NI ($p < 0.0001$) groups. Besides that, we identified the presence of an area of necrosis in the liver of the INT group, however, this presence was not observed in the others groups. No statistical differences from the splenic and nephrotic histopathological analyses were shown between the analyzed groups (Figure 2B).

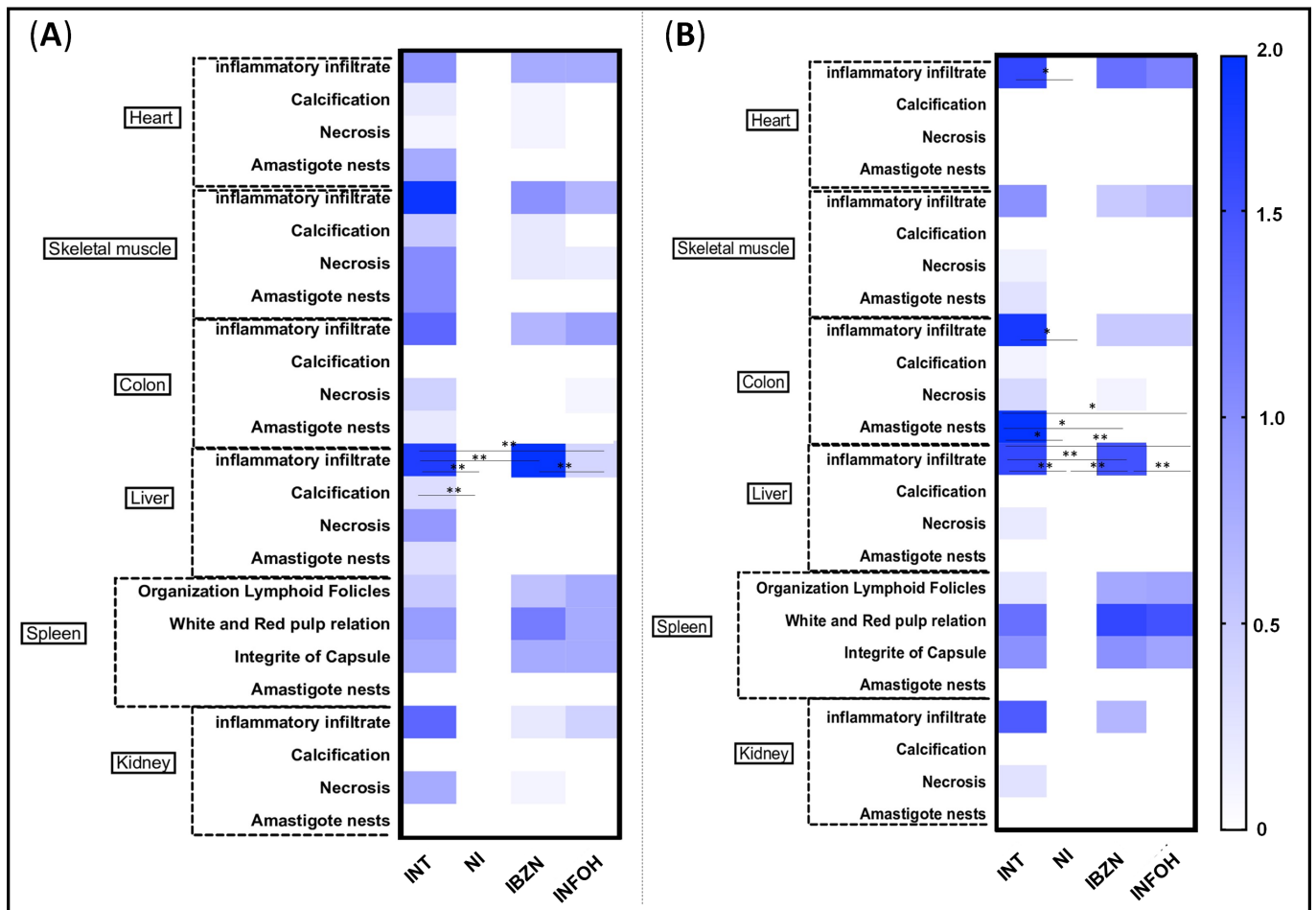


FIGURE 2- Histopathological analysis of the organs and tissues in both murine models (Swiss and C57Bl/6). (A): Histopathological analysis in Swiss mice; (B): Histopathological analysis in C57Bl/6 mice; INT: infected and non-treated group, only vehicle; NI: non-infected group, only vehicle; IBZN: infected and treated with benznidazole; INFOH: infected and treated with hydroxymethylnitrofurazone; Analysis of variance by Student's t-test or one-way ANOVA, with Tukey's post-hoc correction in GraphPad Prism v.7. Differences of $p < 0.05$ were considered significant.*Statistically significant differences ($p \leq 0.05$); **Statistically significant differences ($p \leq 0.005$).

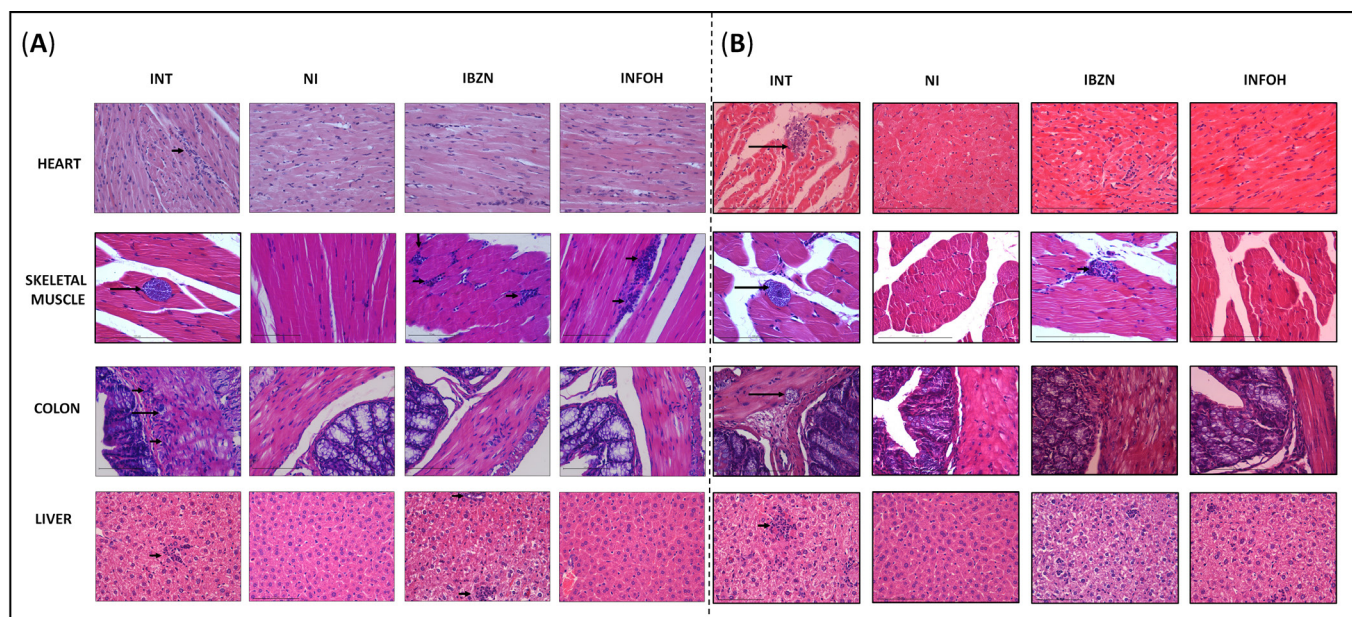


FIGURE 3 - Representative histopathological photography of the heart (H&E, 400X), skeletal muscle (H&E, 400X), colon (H&E, 400X), and liver (H&E, 400X) in two different murine models (Swiss and C57Bl/6). (A): Representative histopathological photography in Swiss mice; (B): Representative histopathological photography in C57Bl/6 mice; INT: infected and non-treated group, only vehicle; NI: non-infected group, only vehicle; IBZN: infected and treated with benznidazole; INFOH: infected and treated with hydroxymethylnitrofurazone; long arrows: presence of amastigote nest; short arrows: inflammatory infiltrates.

In 2018, during indeterminate chronic stage, the NFOH was utilized by 60 days (150 mg/kg) and didn't exhibit any injury in the histopathological analysis of the hepatic and nephrotic tissue, confirmed with association of the hepatic-nephron biochemical analysis, AST and ALT, that presented normal levels³. The histopathological study identified that NFOH (150 mg/kg/day – 60 days of treatment) is able to reduce the intensity of tissue amastigote and infiltrate inflammatory compared to BZN (100 mg/kg) in the indeterminate chronic stage of murine Chagas disease (Y strain, TcII). Moreover, in this study, the authors assessed the effect of NFOH to prevent the parasitaemia reactivation after long-term of treatment, that occurred by drug-induced immunosuppression of *T. cruzi* experiment³. Here, NFOH was able to decrease parasitemia blood during treatment phase, and also avoided parasitic reactivation (after immunosuppression period) in 100% of the animals. In addition, NFOH treatment reduced tissue damage caused by the parasite, as well as observed absence of amastigote nests in all tissues (100%) histologically evaluated, results analogous to BZN-treated mice (100%

parasite absence in blood and tissues: trypomastigote and amastigote forms). Due to promising anti-*T. cruzi* activity, in both Chagas disease stages, as well as its non-hepatotoxicity effect during long-term of treatment (60 days) and high dose concentrations (150 mg/kg) the literature proposes that an NFOH combination with BNZ results in potent antiparasitic activity with less tissue damage than common treatments (Ribeiro *et al.*, 2020; Cortez-Maya *et al.*, 2019; Scarim *et al.*, 2018b; Scarim, Chung, 2019). These findings are interesting and deserve further investigation.

CONCLUSION

In conclusion, NFOH reduced in 100% the parasitaemia through short-term treatment in acute Swiss and C57Bl/6 murine experiments. The histopathological results displayed that NFOH decreased in 100% the amastigote nests in all animal organs (similar to BZN). Moreover, we also verified hepatic inflammation (hepatotoxicity) in NFOH-treated mice. Thus, further studies need to be carried out to determine the authentic

activity of NFOH, whether it acts as a trypanocidal or trypanostatic, thus being a possible alternative for the safe treatment of Chagas disease.

ACKNOWLEDGMENT

The authors would like to thank the Fundação de Amparo à Pesquisa do Estado de São Paulo (FAPESP - 2016/10847-9) by the research fellowships assistance. This work was financed in part by the Coordenação de Aperfeiçoamento Pessoal de Nível Superior - Brasil (CAPES) - finance code: 001.

AUTHOR CONTRIBUTIONS

C.B.S., C.R.A., R.F., L.M.A., V.I.S., J.A.R., and C.M.C., designed the experiments and analyzed the data. C.B.S., C.R.A., R.F., L.M.A., and V.I.S., performed the experiments. C.B.S., wrote the manuscript, with input from C.R.A., R.F., L.M.A., V.I.S., J.A.R., and C.M.C. All authors reviewed the manuscript.

CONFLICTS OF INTEREST

The authors declare no conflict of interest.

REFERENCES

Andrade AL de, Zicker F, Oliveira RM de, Almeida Silva S, Luquetti A, Travassos LR, et al. Randomised trial of efficacy of benznidazole in treatment of early *Trypanosoma cruzi* infection. *Lancet*. 1996;348(9039):1407-13. doi:10.1016/S0140-6736(96)04128-1.

Andrade MC, Oliveira MDF, Nagao-Dias AT, Coêlho IC, Cândido D da S, Freitas EC, et al. Clinical and serological evolution in chronic Chagas disease patients in a 4-year pharmacotherapy follow-up: a preliminary study. *Rev Soc Bras Med Trop*. 2013;46(6):776-778. doi:https://doi.org/10.1590/0037-8682-1646-2013.

Castro JA, de Mecca MM, Bartel LC. Toxic side effects of drugs used to treat Chagas' disease (American trypanosomiasis). *Hum Exp Toxicol*. 2006;25:471-79.

Cortez-Maya S, Moreno-Herrera A, Palos I, Rivera G. Old Antiprotozoal Drugs: Are They Still Viable Options for Parasitic Diseases or New Options for Other Diseases?. *Curr Med Chem*. 2020;27(32):5403-5428.

Chagas C. Nova tripanozomíase humana. Estudos sobre a morfologia e o ciclo evolutivo do *Schizotrypanum cruzi* n. gen. n. sp., agente etiológico de uma nova entidade mórbida do homem. *Mem Inst Oswaldo Cruz*. 1909;1(2):159-218.

Chung MC, Guido RVC, Martinelli TF, Gonçalves MF, Polli MC, Botelho KCA, et al. Synthesis and *in vitro* evaluation of potential antichagasic hydroxymethylnitrofurazone (NFOH-121): A new nitrofurazone prodrug. *Bioorg Med Chem*. 2003;11(22):4779-83.

Davies C, Cardozo RM, Negrette OS, Mora MC, Chung MC, Basombrio MA. Hydroxymethylnitrofurazone is active in a murine model of Chagas' disease. *Antimicrob Agents Chemother*. 2010;54(9):3584-9.

Davies C, Dey N, Negrette OS, Parada LA, Basombrio MA, Garg NJ. Hepatotoxicity in Mice of a Novel Antiparasite Drug Candidate Hydroxymethylnitrofurazone: A Comparison with Benznidazole. *PLoS Negl Trop Dis*. 2014;8(10):e3231.

DNDi. Drugs for Neglected Diseases initiative (DNDi), Neglected Tropical Diseases. <https://www.dndi.org/diseases-projects/chagas/>. (Accessed 25 February 2021). 2018.

Ekins S, de Siqueira-Neto JL, McCall LI, Sarker M, Yadav M, Ponder EL, et al. Machine Learning Models and Pathway Genome Data Base for *Trypanosoma cruzi* Drug Discovery. *PLoS Negl Trop Dis*. 2015;9(6):e0003878

Fernandes CD, Tiecher FM, Balbinot MM, Liarte DB, Scholl D, Steindel M, et al. Efficacy of benznidazol treatment for asymptomatic chagasic patients from state of Rio Grande do Sul evaluated during a three years follow-up. *Mem Inst Oswaldo Cruz*. 2009;104(1):27-32. doi:https://doi.org/10.1590/S0074-02762009000100004.

Fernandez ML, Marson ME, Ramirez JC, Mastrantonio G, Schijman AG, Altcheh J, et al. Pharmacokinetic and pharmacodynamics responses in adult patients with Chagas disease treated with a new formulation of benznidazole. *Mem Inst Oswaldo Cruz*. 2016;111(3):218-21. doi:https://doi.org/10.1590/0074-02760150401.

Guido RVC, Ferreira EI, Nassute JC, Varanda EA, Chung MC. Diminuição da atividade mutagênica do pró-fármaco NFOH-121 em relação ao nitrofurazone (nitrofurazona). *Rev Ciênc Farm*. 2001;22(2):319-33.

Hasslocher-Moreno AM, do Brasil PEAA, de Sousa AS, Xavie SS, Chambela MC, Sperandio da Silva GM. Safety of benznidazole use in the treatment of chronic Chagas' disease. *J Antimicrob Chemother*. 2012;67(5):1261-66. DOI:https://doi.org/10.1093/jac/dks027

Lidani KCF, Andrade FA, Bavia L, Damasceno FS, Beltrame MH, Messias-Reason IJ, et al. Chagas Disease: From

Discovery to a Worldwide Health Problem. *Front Public Health*. 2019;7:1-13. DOI:10.3389/fpubh.2019.00166

Maya JD, Orellana M, Ferreira J, Kemmerling U, López-Muñoz R, Morello A. Chagas disease: present status of pathogenic mechanisms and chemotherapy. *Biol Res*. 2010;43(3):323-31. doi:https://doi.org/10.4067/S0716-97602010000300009.

Nogueira-Filho MAF, Carvalho EC, De Campos ML, Machado DVP, Davanço MG, Pestana KC, et al. Pharmacokinetics of Hydroxymethylnitrofurazone and Its Parent Drug Nitrofurazone in Rabbits. *Drug Metab Lett*. 2013;7(1):58-64.

Ribeiro V, Dias N, Paiva T, Hagström-Bex L, Nitz N, Pratesi R, et al. Current trends in the pharmacological management of Chagas disease. *Int J Parasitol Drugs Drug Resist*. 2020;10(12):7-17.

Scarim CB, Chung CM. Nitroheterocyclic derivatives: privileged scaffold for drug development against Chagas disease. *Med Chem Res*. 2019;28(12):2099-108.

Scarim CB, de Andrade CR, da Rosa JA, dos Santos JL, Chung MC. Hydroxymethylnitrofurazone treatment in indeterminate form of chronic Chagas disease: Reduced intensity of tissue parasitism and inflammation—A histopathological study. *Int J Exp Pathol*. 2018a;99(5):236-48.

Scarim CB, Jornada DH, Chelucci RC, De Almeida L, Dos Santos JL, Chung CM. Current advances in drug discovery for Chagas disease. *Eur J Med Chem*. 2018b;155:824-838.

Serafim EOP, Silva ATA, Moreno AH, Vizioli EO, Ferreira EI, Peccinini RG, et al. Pharmacokinetics of hydroxymethylnitrofurazone, a promising new prodrug for chagas' disease treatment. *Antimicrob Agents Chemother*. 2013;57(12):6106-9.

Silva GMS Da, Mediano MF, Alvarenga Americano do Brasil PE, da Costa Chambela M, da Silva JA, de Sousa AS, et al. A clinical adverse drug reaction prediction model for patients with chagas disease treated with benznidazole. *Antimicrob Agents Chemother*. 2014;58(1):6371-77. doi:10.1128/AAC.02842-14.

Sosa-Estani S, Segura E, Ruiz A, Velazquez E, Porcel B, Yampotis C. Efficacy of chemotherapy with benznidazole in children in the indeterminate phase of Chagas' disease. *Am J Trop Med Hyg*. 1998;59(4):526-9.

Soy D, Aldasoro E, Guerrero L, et al. Population pharmacokinetics of benznidazole in adult patients with Chagas disease. *Antimicrob Agents Chemother*. 2015;59(6):3342-49. doi:https://doi.org/10.1128/AAC.05018-14.

Received for publication on 07th July 2020

Accepted for publication on 04th July 2021